Mechanics of Composite Materials, Vol. 47, No. 2, May, 2011 (Russian Original Vol. 47, No. 2, March-April, 2011)

VISCOELASTIC BEHAVIOR AND DURABILITY OF STEEL-WIRE - REINFORCED POLYETHYLENE PIPES UNDER A HIGH INTERNAL PRESSURE

S. G. Ivanov,*[1] A. N. Anoshkin[2], and V. Yu. Zuyko[2]

Keywords: *polyethylene pipe, steel wire skeleton, viscoelasticity, elastoplasticity, short-term strength, durability*

The strength tests of steel-wire-reinforced polyethylene pipe specimens showed that, under a constant internal pressure exceeding 80% of their short-term ultimate pressure, the fracture of the specimens occurred in less than 24 hours. At pressures slightly lower than this level, some specimens did not fail in a year and a half. The analytical model developed for describing the mechanical behavior of such pipes considers that polyethylene is viscoelastic and steel is elastoplastic. This allows one to evaluate their short-term strength as well as their durability under a high internal pressure. The experimental results obtained in strength tests are explained by the redistribution of stresses between the two materials of the reinforced pipe. Calculations were carried out using the MathCAD software.

Results of Pipe Tests

The technology of polyethylene pipes reinforced with a steel wire skeleton has been developed and introduced for the first time at the "Mepos" company (Ekaterinburg, Russia). At present, such pipes are manufactured by several Russian companies, in particular, "Polimak" JSC (Ekaterinburg) and "Gazprom Transgaz Stavropol" LLC (Stavropol). The wires in the skeleton are fastened by spot welding at their intersection points (Fig. 1). The results of a finite-element modeling of stresses in the wire skeleton and in the polyethylene body of pipe specimens, obtained in tests for the short-term strength, are discussed in [1].

The tests for the short- and long-term strength of pipe specimens manufactured by "Polimak" JSC, with an outer diameter of 140 mm, including the nonreinforced thickened zone of a butt weld of polyethylene, were carried out at the Perm

[1]University of Twente, Netherlands
[2]Perm State Technical University, Russia
*Corresponding author; e-mail: ivanovsgen@gmail.com.

Translated from Mekhanika Kompozitnykh Materialov, Vol. 47, No. 2, pp. 277-288, March-April, 2011. Original article submitted September 23, 2010.

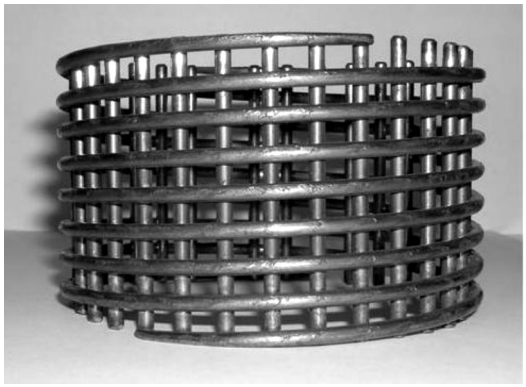

Fig. 1. Steel skeleton of a reinforced plastic pipe.

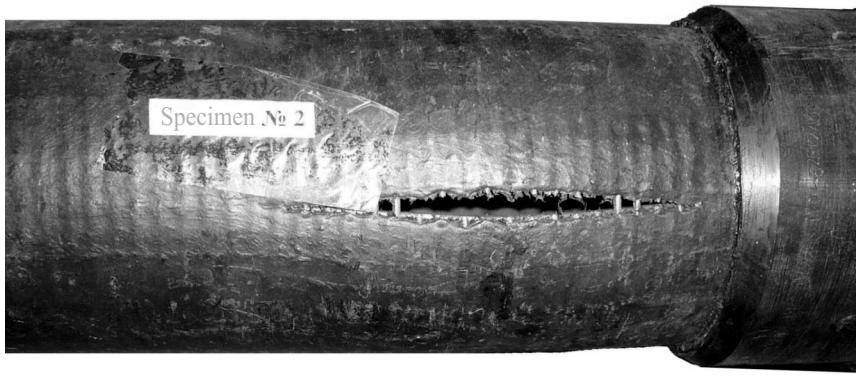

Fig. 2. Specimen of a reinforced pipe after short-time tests under internal pressure.

TABLE 1. Results of Tests on Pipe Specimens for the Long-Term Strength

Specimen	p_{const}, MPa	$p_{const}/p_{lim} \cdot 100\%$	Time to failure and its character
4	9.8	87.5	1 h, a longitudinal crack with a broken reinforcement
5	9.2	82	21 h, a longitudinal crack with a broken reinforcement
6	8.2	73	Did not failed in 570 days ($1.37 \cdot 10^4$ h)
7	7.5	67	Did not failed in 630 days ($1.51 \cdot 10^4$ h)
8	6.0 (during 298 days ($7.15 \cdot 10^3$ h), then increased to 8.4	54 (during 298 days), then increased to 75	Did not failed in 298 days at a pressure of 6.0 MPa; on increasing to 8.4 MPa, failed in 11 hours at a polyethylene seem

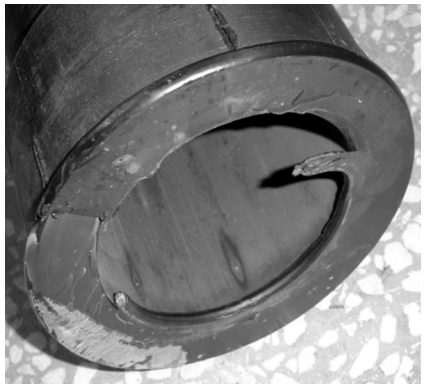

Fig. 3. Failure of specimen 8 (according to Table 1) along a welded unreinforced joint.

State Technical University. Specimens 1, 2, and 3, loaded with an internal pressure at a rate of 10 MPa/min, in short-term strength tests, failed at 10, 13, and 10.5 MPa, respectively. The ultimate pressure describing the short-term strength of the pipe, averaged over three specimens, was p_{lim} = 11.2 MPa. A typical pattern of failure of a pipe specimen is illustrated in Fig. 2, where a longitudinal crack with broken circular coils of the reinforcement is shown.

In tests for the long-term strength (Table 1), the internal pressure grew to a certain level p_{const} and was then maintained at this level up to failure of specimens. We should note that, at a loading level higher than a certain value (~80% of the short-term strength), the failure occurred within 24 hours with the break of reinforcement, as in the case of tests for the short-term strength (see Fig. 2). However, at a pressure below this level, specimens 6 and 7 did not fail even in one year and a half. The purpose of the present study is to explain this fact and to predict the long-term strength of such pipes at high loading levels.

Taking into account the fact that polyethylene is viscoelastic, but the greater part of load is taken up by the steel wire, we may assume that the long-term strength of the pipes at high load levels, in the course of time, is caused by redistribution of the load between the polyethylene and the wire wound in the circumferential direction.

The destruction character of specimen 8 indicates that, at load levels lower than ~80% of the short-term strength, for the given standard-size pipes, the creep failure of polyethylene in the axial direction can occur in the region of a nonreinforced thickened joint (Fig. 3). For predicting the failure according to this mechanism, competing with the break of the circular reinforcement, data on the nonlinear behavior of polyethylene in creep up to failure are necessary.

Properties and Deformation of the Wire in the Circular Direction

The wire skeleton of a pipe of outer diameter 140 mm had the following parameters: wire diameter $2r$ = 3 mm, median diameter of the wire ring $2R$ = 134 mm, and the winding step a = 8 mm. Figure 4 shows tension diagrams of the wire in the initial state and of a wire taken out of the pipe, i.e., weakened by contact welding.

For our calculations, we used a simple piecewise linear two-section approximation of the tension diagram (Fig. 5). The elastic region is followed by a region of a constant stress $\sigma = \sigma_{\max}$ at a strain $\varepsilon_s \le \varepsilon \le \varepsilon_{\text{lim}}$. Here, $\varepsilon_s = \sigma_{\max}/E$, where E is the elastic modulus of steel. The parameters $\sigma_{\max}$ and ε_{lim} are chosen so that to describe the weakest wire, since its destruction leads to the failure of neighboring wires and to the formation of a longitudinal crack. It is seen that the contact welding affects the tension diagram significantly.

Upon twisting the wire into a ring, some part of the material occurs in the region of plastic deformation. The longitudinal deformation of bending due to winding $|\varepsilon| \le r/R$ = 0.022 is distributed linearly over the cross section of wire. Using

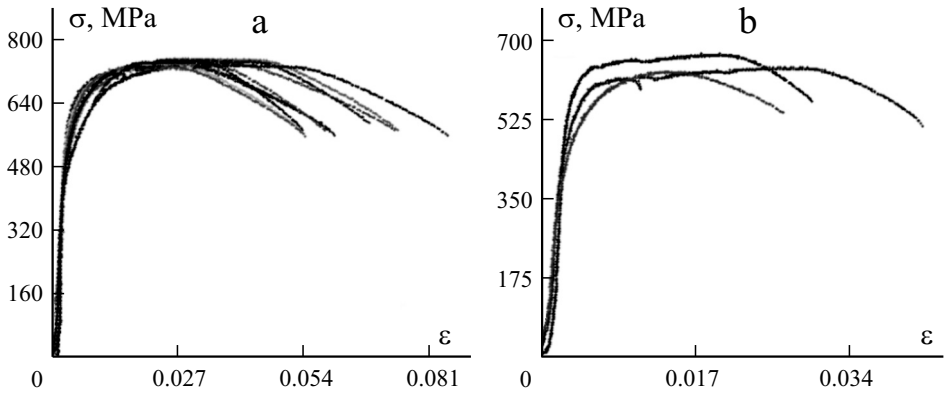

Fig. 4. Deformation diagrams of the wire in the initial state (a) and after the contact welding (b).

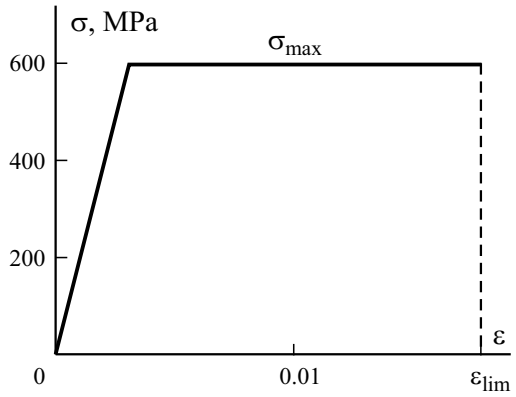

Fig. 5. Approximation of the deformation diagram of wire in active loading.

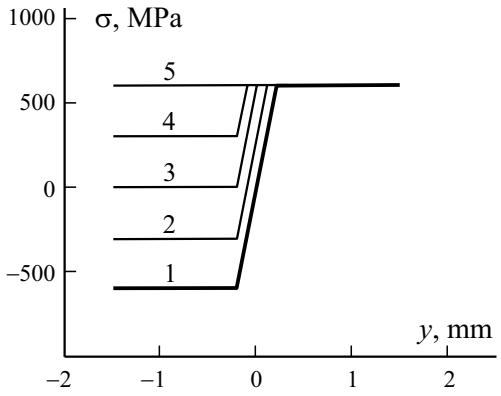

Fig. 6. Distribution of the stress across the wire thickness at averaged strains equal to 0 (1), $\varepsilon_s/2$ (2), ε_s (3), $3\varepsilon_s/2$ (4), and $2\varepsilon_s$ (5).

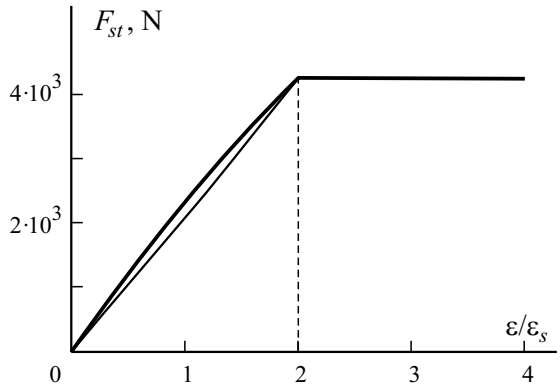

Fig. 7. Tensile force F_{st} as a function of the strain ε averaged over the cross section of the wire.

the tension diagram of the wire (see Fig. 4) and assuming that the diagram $\sigma(\varepsilon)$ in compression is similar, we come to a relation between the longitudinal strain of the wire after winding and the coordinate y. At the center of cross section of the wire, $y = 0$. After imposing on the wire the tensile deformation from the internal pressure in the pipe, an elastic unloading occurs in the compressed region of cross section.

Figure 6 shows the distribution of stresses over the cross section of the wire at different values of the average strain (tensile strain from the internal pressure). The distribution of the stresses was described by the piecewise linear function

$$\sigma(y,\varepsilon) = \begin{cases} -\sigma_{\max} + E\varepsilon + f_1\left(E\frac{y}{R} + \sigma_{\max}\right) - f_1\left(E\frac{y}{R} + E\varepsilon - \sigma_{\max}\right), & 0 \le \varepsilon \le 2\varepsilon_s, \\ \sigma_{\max}, & \varepsilon > 2\varepsilon_s, \end{cases} \tag{1}$$

$$f_1(x) = \begin{cases} 0, & x < 0, \\ x, & x \ge 0, \end{cases}$$

where ε is the strain averaged over the cross section.

Integrating Eq. (1) over the cross-sectional area of the wire, we obtain a relation between the force F_{st} which stretches the wire and ε (Fig. 7).

This relation was approximated by the piecewise linear function

$$F_{\text{st}}(\varepsilon) = \frac{E}{2} A_{\text{st}}\left(\varepsilon - f_1(\varepsilon - 2\varepsilon_s)\right) = \begin{cases} \frac{E}{2} A_{\text{st}}\varepsilon, & \varepsilon < 2\varepsilon_s, \\ EA_{\text{st}}\varepsilon_s = \sigma_{\max}, & \varepsilon \ge 2\varepsilon_s. \end{cases} \tag{2}$$

Viscoelastic Deformation of Polyethylene

In [2], the viscoelastic properties of the polyethylene used for pipes manufactured by winding of a polyethylene tape reinforced with a steel wire were determined from creep tests at six levels of constant stresses, from 4 to 14 MPa.

The circumferential strain in the reinforced pipes before origination of a crack was rather small, of an order of magnitude 2%. For such a level of strains, the nonlinear viscoelastic behavior of polyethylene was approximated in [2] by the linear viscoelastic model

TABLE 2. Parameters of the Linear Viscoelastic Model [2] and the Calculated Values of the Relaxation Kernel in Uniaxial Tension

Parameter	$i = 0$	$i = 1$	$i = 2$	$i = 3$	$i = 4$	$i = 5$
τ_i, s		10	500	$5 \cdot 10^3$	$5 \cdot 10^4$	$5 \cdot 10^5$
G_i, MPa	470	509	477	359	367	314
G_0/G_i		0.925	0.99	1.31	1.28	1.50
$1/\beta_i$		5.3	330	$3.49 \cdot 10^3$	$3.86 \cdot 10^4$	$3.97 \cdot 10^5$
A_i/β_i		0.473	0.184	0.102	0.054	0.037

$$\varepsilon_{ij}(t) = \frac{\sigma_{kk}(t)\delta_{ij}}{9K_0} + \frac{1}{2G_0}\left[s_{ij}(t) + \int_0^t K_G(t-\tau) s_{ij}(\tau)\, d\tau \right], \tag{3}$$

where s_{ij} are components of the stress deviator, $s_{ij} = \sigma_{ij} - \dfrac{\sigma_{kk}}{9K_0}\delta_{ij}$.

The kernel $K_G(t)$ in Eq. (3) was taken as a sum of five exponents:

$$K_G(t) = \sum_{i=1}^{5} \frac{G_0}{G_i} \cdot \frac{1}{\tau_i} \exp\left(\frac{t}{\tau_i} \right). \tag{4}$$

The values of τ_i and G_i in Eq. (4), found by the method of least squares, are presented in Table 2.

For the case of uniaxial tension, we have from relation (3)

$$\varepsilon_{11}(t) = \frac{1}{E_0}\left[\sigma_{11}(t) + \int_0^t K(t-\tau)\sigma_{11}(\tau)\, d\tau \right]. \tag{5}$$

The instantaneous modulus E_0 can be expressed in terms of the constant G_0 and the Poisson ratio $\nu = 0.42$ (taken from [2]): $E_0 = 2(1+\nu)G_0$.

The parameters of the kernel $K(t)$ in Eq. (5) can be expressed in terms of parameters of the kernel $K_G(t)$:

$$K(t) = \frac{E_0}{3G_0} K_G(t), \; K_G(t) = \sum_{i=1}^{5} B_i \exp(-\gamma_i t), \; B_i = \frac{E_0}{3G_i} \cdot \frac{1}{\tau_i}, \; \gamma_i = 1/\tau_i .$$

The functional inverse to (5), with subscripts omitted, is

$$\sigma(t) = E_0\left[\varepsilon(t) - \int_0^t \Gamma(t-\tau)\varepsilon(\tau)\, d\tau \right], \quad \Gamma(t) = \sum_{i=1}^{5} A_i \exp(-\beta_i t). \tag{6}$$

The constants of the kernel $\Gamma(t)$ in (6) were calculated from those of the kernel $K(t)$ by using the known relations [3]

$$\sum_{i=1}^{5} \frac{A_i}{\beta_i - \gamma_j} = 1, \quad \sum_{i=1}^{5} \frac{B_i}{\beta_j - \gamma_i} = 1, \; j = 1, \ldots, 5, \tag{7}$$

and their values are also presented in Table 2.

Let us find what estimate for the level of axial strain ε^* reached in the polyethylene joint by the instant of failure or the end of the tests is given by the linear model. For the diameter of butt joint 164 mm, the calculations by Eq. (5) give the following values of ε^* for specimens 4-8 (see Table 1): 2.4, 3.3, 3.8, 3.5, and 3.6%, respectively.

As seen, the strain level in specimen 8 is higher than in other ones, except for specimen 6, which did not fail. However, the distinction is insignificant and apparently lies within the statistical straggling of the ultimate strain for a welded polyethylene joint. As already mentioned, for predicting the failure in a nonreinforced thickened joint, it is necessary to have data on the nonlinear behavior of polyethylene in creep up to failure, as well as data on the strength of welded joints.

Viscoelastoplastic Deformation of a Reinforced Pipe

Let us consider the deformation of a pipe under an internal pressure according to a simplified model, assuming that the circular reinforcement is preliminary deformed elastoplastically and the polyethylene is linearly viscoelastic (the presence of the longitudinal reinforcement is neglected since the load from the internal pressure is taken up mainly by the circular reinforcement).

Let us now examine the equilibrium of a nonuniform ring of rectangular cross section of width a (a is the distance between wire coils in the pipe), thickness h, and inner radius R_1, loaded with an internal pressure p. The ring contains a steel wire ring with a median radius R and cross-sectional area $A_{st} = \pi r^2$; the radius of the wire is r. The cross-sectional area of the ring occupied by polyethylene is $A_{pe} = ha - A_{st}$. The equilibrium equation of such a ring has the form

$$pR_1 a = F_{st}(\varepsilon) + F_{pe}(\varepsilon), \tag{8}$$

where $F_{st}(\varepsilon)$ is the force falling on the steel wire (2), and $F_{pe}(\varepsilon)$ is that falling on the polyethylene part of the ring.

For simplicity, we assume that the strain in the polyethylene ring is homogeneous and equal to the average cross-sectional strain in the wire. Thereby we pass on to the consideration of tension of a nonuniform rod with a steel core, assuming that both the steel and the polyethylene in this core are in a uniaxial stress state. Let us designate the longitudinal strain of the core by ε. $F_{st}(\varepsilon)$ is determined by Eq. (2), whereas $F_{pe}(\varepsilon)$, with account of Eqs. (6), is given by

$$F_{pe}(\varepsilon) = A_{pe}E_0\left[\varepsilon(t) - \int_0^t \Gamma(t-\tau)\varepsilon(\tau)\,d\tau\right]. \tag{9}$$

Let us consider the case $\varepsilon \le 2\varepsilon_s$. Equation (8), with account of Eqs. (2) and (9), can be put into the form

$$p(t) = k_{st}\varepsilon(t) + k_{pe}\left[\varepsilon(t) - \int_0^t \Gamma(t-\tau)\varepsilon(\tau)\,d\tau\right] = k\left[\varepsilon(t) - \int_0^t \Gamma_1(t-\tau)\varepsilon(\tau)\,d\tau\right], \tag{10}$$

where

$$k_{st} = \frac{A_{st}E}{2R_1 a}\ k_{pe} = \frac{A_{pe}E_0}{R_1 a}\ k = k_{st} + k_{pe},\ \ \Gamma_1(t) = \frac{k_{pe}}{k}\Gamma(t).$$

At $\varepsilon \le 2\varepsilon_s$, the deformation can be presented as the functional inverse to (10)

$$\varepsilon_1(t) = \frac{1}{k}\left(p(t) + \int_0^t \mathrm{K}_1(t-\tau)p(\tau)\,d\tau\right), \tag{11}$$

where $\Gamma_1(t)$ is the resolvent of the kernel $K_1(t)$; the parameters of the kernels are connected by relations similar to Eqs. (7). The time at which $\varepsilon_1(t_s) = 2\varepsilon_s$ is designated by t_s.

Then, Eq. (8) can be written as

$$p(t) - \frac{F_{st}(\varepsilon(t))}{R_1 a} = k_{pe}\left[\varepsilon(t) - \int_0^t \Gamma(t-\tau)\varepsilon(\tau)\,d\tau\right]. \tag{12}$$

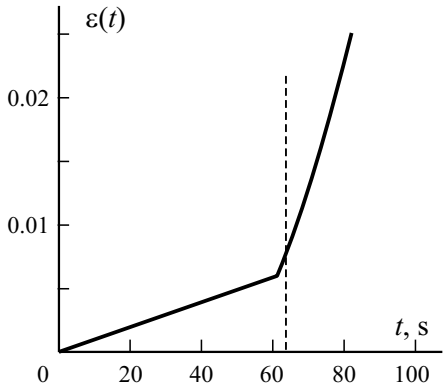

Fig. 8. Circumferential strain ε as a function of time t at the constant loading rate of the pipe $\dot{p}(t) =$ 10 MPa/min.

For the case $\varepsilon > 2\varepsilon_s$, we have from Eq. (11)

$$\varepsilon(t) = \frac{1}{k_{\text{pe}}}\left[\Delta p(t) + \int_0^{t_s} \mathrm{K}(t-\tau)(p(\tau) - k_{\text{st}}\varepsilon_1(\tau))d\tau + \int_{t_s}^{t} \mathrm{K}(t-\tau)\Delta p(\tau)d\tau\right], \tag{13}$$

where $\Delta p(t) = p(t) - 2\varepsilon_s k_{\text{s}}$.

Example of Estimation of the Short-Term Strength and Durability of a Reinforced Pipe at a High Pressure

Let us consider the example of calculation of a pipe of outer diameter 140 mm with the following geometrical parameters: $R_1 = 57$ mm, $R = 67$ mm, $h = 13$ mm, $a = 8$ mm, and $2r = 3$ mm. The lower estimate for the ultimate pressure upon its short-term increase can be found from Eq. (8) by neglecting the second term in the right-hand side, which is responsible for the contribution of polyethylene to the load-carrying ability of the pipe:

$$p_{\text{lim}(st)} = 2\varepsilon_s k_{st}$$

For the parameter $\sigma_{\max} = 600$ MPa of the approximating diagram of the steel wire (see Fig. 4), this estimate gives $p_{\text{lim(st)}} = 9.3$ MPa. At a lower pressure, no destruction due to the redistribution of stresses is possible. Now, we will take into account the contribution of polyethylene to the load-carrying ability of the pipe. As a criterion of exhaustion of its load-carrying ability, we choose

$$\varepsilon(t) \le \varepsilon_{\text{lim}}, \tag{14}$$

where $\varepsilon_{\text{lim}} = 1.8\%$.

Let us consider the loading at a constant speed $\dot{p} = 10$ MPa/min = 1/6 MPa/s. Using Eqs. (11) and (13) and criterion (14), we find the ultimate pressure at a constant rate of its increase: $p_{\text{lim}} = 12.6$ MPa. In this case, the contribution of the steel wire to the magnitude of breaking pressure in short-term loading up to failure makes 74%. The time-dependent strain of the pipe at a constant rate of loading by internal pressure is illustrated in Fig. 8.

The kink in the strain diagram is explained by the kink in the calculated diagram for the steel wire. The pressure at this point is $p(t_s) = 10.2$ MPa.

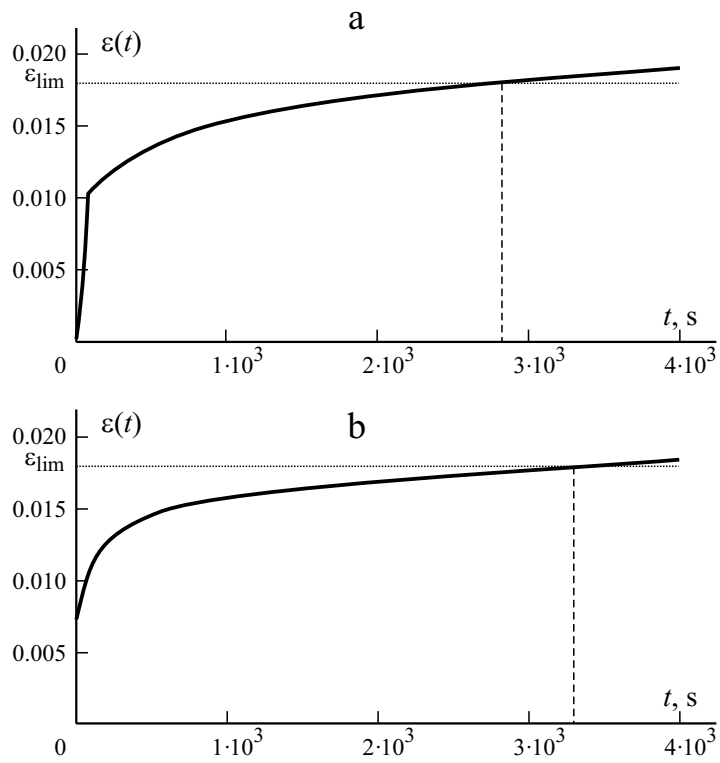

Fig. 9. Deformation of the wire in long-term strength tests at p_{const1} = 10.8 MPa (a) and p_{const2} = 10.3 MPa (b).

Now, we will consider the deformation of the steel wire during long-term tests, when the pressure is raised with a constant rate $\dot{p}$ up to a given level p_{const} and then is held constant at this level up to failure. Analytically, the pressure in such tests is described by the piecewise linear function of time

$$p(t) = \dot{p}\left[t - f_1\left(t - \frac{p_{\text{const}}}{\dot{p}}\right)\right]. \tag{15}$$

Inserting Eq. (15) into Eq. (11), we obtain a relation between the strain and time for $\varepsilon \le 2\varepsilon_s$. In calculating the time t_s at which the strain reaches the level $2\varepsilon_s$, we employ Eq. (13) to construct the time–strain relationship at $\varepsilon > 2\varepsilon_s$. The relationships obtained are shown in Fig. 9a for p_{const1} = 10.8 MPa and Fig. 9b for p_{const2} = 10.3 MPa. Related to the estimated ultimate pressure p_{lim} = 12.6 MPa in short-term tests, these pressure levels are practically equal:

$$\frac{p_{\text{const1}}}{p_{\text{lim}}} \cdot 100\% = 86\%, \quad \frac{p_{\text{const2}}}{p_{\text{lim}}} \cdot 100\% = 82\%.$$

Using then criterion (14), we come to a predicted durability T_1 = 47 min in the first case and T_2 = 18 h in the second one. All the calculations were carried out in the MathCAD package.

Conclusions

The analytical model suggested for estimating the short-term strength and durability of highly loaded pipes reinforced with a steel skeleton yields quite good results in comparison with experimental data.

The calculated short-term strength is somewhat overestimated compared with the experimental one: 12.6 MPa against 11.2 MPa, averaged over three tests. For a more accurate estimate, more complete data are needed on the deformation of a wire weakened by contact welding. We should also point to the wide scatter of experimental data on the short-term strength.

REFERENCES

1. S. G. Ivanov, L. L. Strikovskii, M. A. Gulyaeva, and V. Yu. Zuiko, "Modeling the mechanical behavior of metal-reinforced plastic pipes under internal pressure," Mech. Compos. Mater., **41**, No. 1, 39-48 (2005).
2. M. P. Kruijer, L. L. Warnet, and R. Akkerman, "Modeling of the viscoelastic behavior of steel-reinforced thermoplastic pipes," Composites: Pt A, **37**, 356-367 (2006).
3. V. V. Moskvitin, Strength of Viscoelastic Materials [in Russian], Nauka, Moscow (1972).